Electronic Supplementary Material (ESI) for Journal of Materials Chemistry B

Supporting Information

Applications of porous organic frameworks (POFs) in detection of nucleic acid and exonuclease I activity

Chan Song,[a,b] Guan-Yao Wang,[a,b] Hui-Zhen Wang,[b,c] Yong-Jian Wang [b,c] and De-Ming Kong*[a,b]

[a] *State Key Laboratory of Medicinal Chemical Biology, College of Chemistry, Nankai University, Tianjin 300071, P R China.*
[b] *Collaborative Innovation Center of Chemical Science and Engineering (Tianjin), Tianjin 300071, China.*
[c] *Key Laboratory of Bioactive Materials (Ministry of Education), College of Life Sciences, Nankai University, Tianjin 300071, China.*
Email: kongdem@nankai.edu.cn; Tel: (+86)-22-23500938; Fax: (+86)-22-23502458

1. Materials

Table S1 The oligonucleotides used in this work.

Olignucleotide	Sequence (5′ to 3′)
P (FAM dye-labeled ssDNA)	GGA AGT GTT GAT AAG ATA-(FAM)
T (complementary target to **P**)	TAT CTT ATC AAC ACT TCC
T1 (single-base mismatched target to **P**)	TAT CTT ATC **T**AC ACT TCC
T2 (two-base mismatched target to **P**)	TAT CTT **T**TC **T**AC ACT TCC
T3 (three-base mismatched target to **P**)	TAT CTT **T**TC **T**AC **T**CT TCC
T4 (non-complementary target to **P**)	CGA GGC GAT GCC GAA CTC GA

2. Synthesis and general characterizations of PAF-6

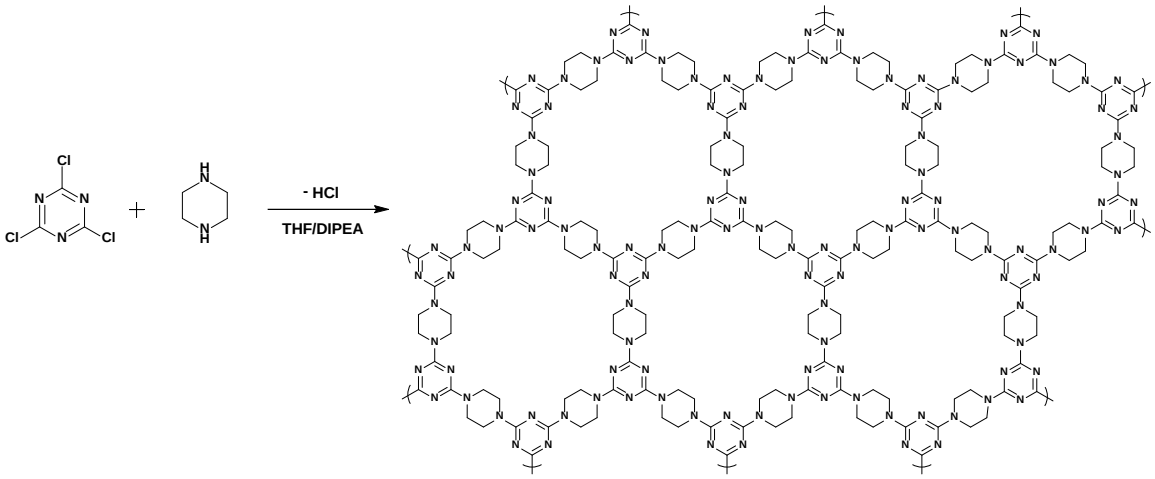

Fig. S1 The synthesis route of PAF-6.

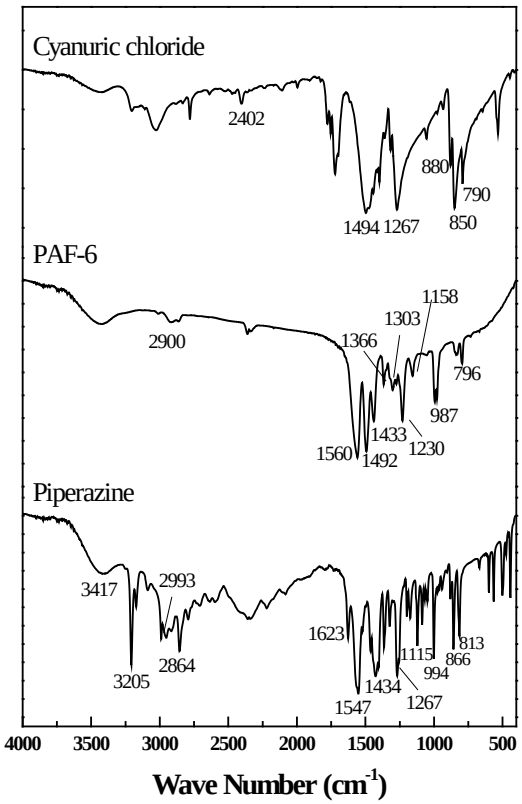

Fig. S2 IR spectra of cyanuric chloride, PAF-6 and piperazine.

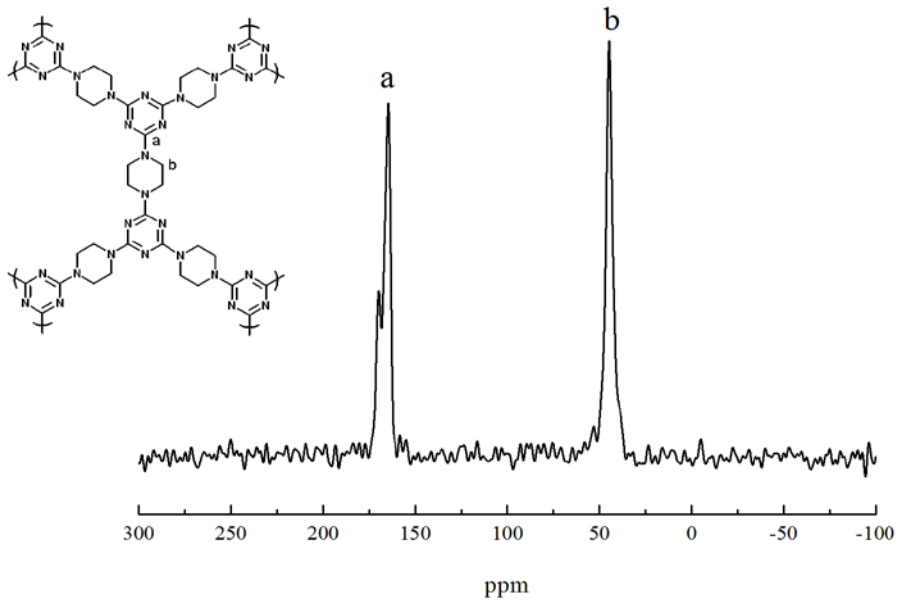

Fig. S3 ^{13}C NMR traces of PAF-6.

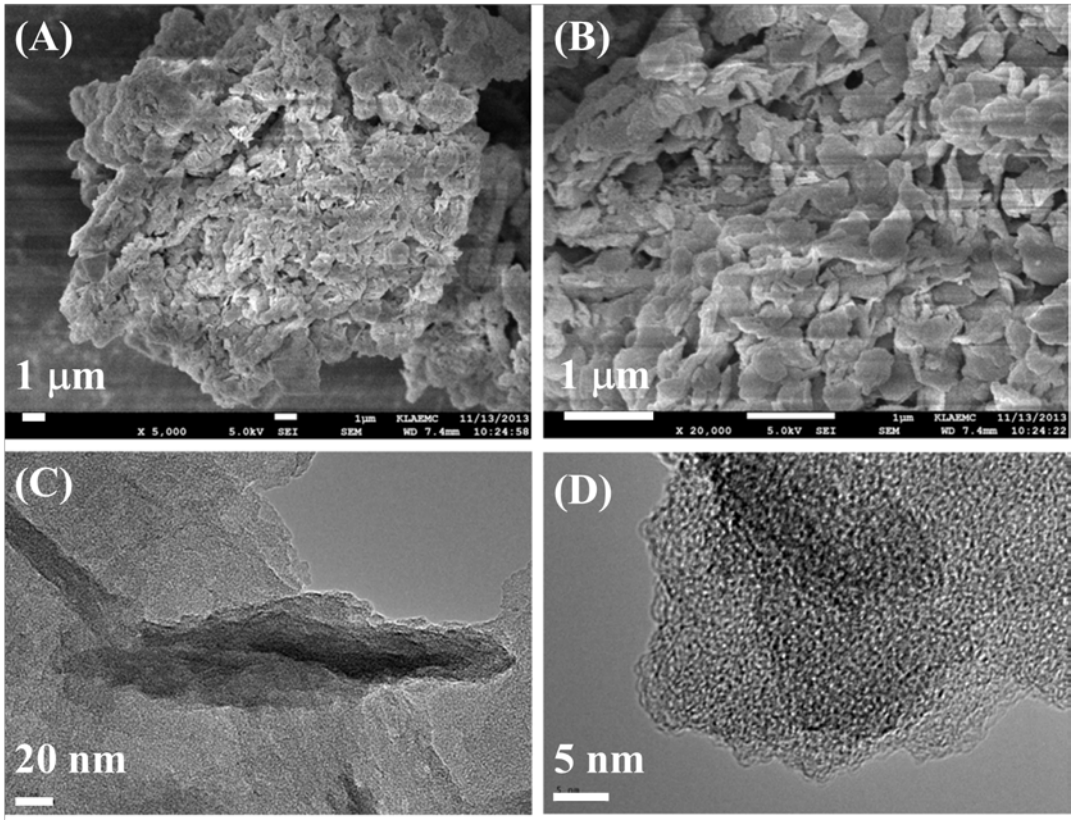

Fig. S4 Typical SEM (A, B) and TEM (C, D) images of PAF-6.

3. Cytotoxicity assay of PAF-6

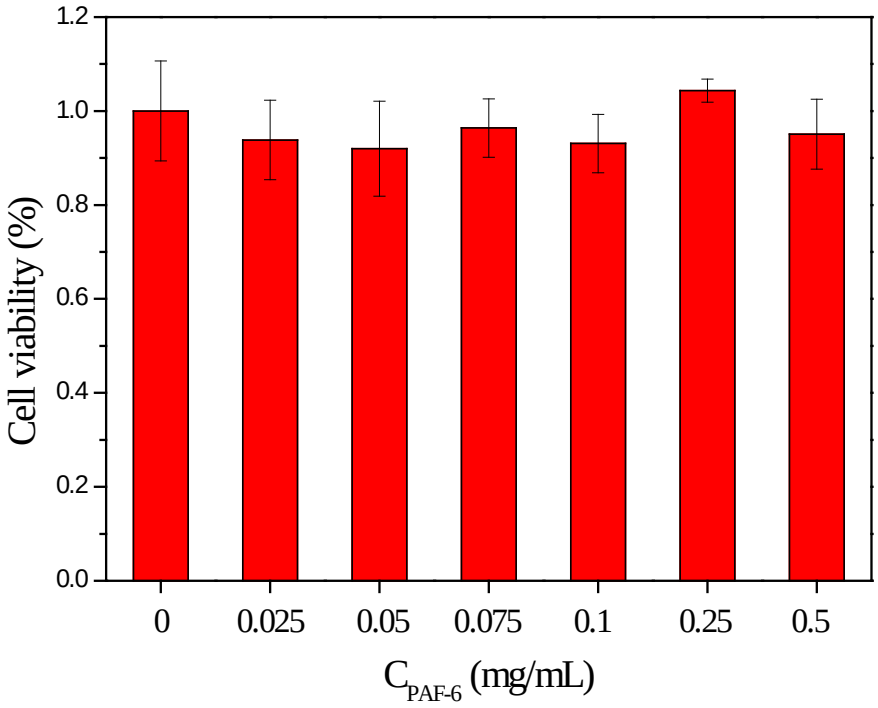

Fig. S5 Cell viability of MDA-MB-231 cells treated with PAF-6 at different concentrations. Each sample was replicated in five wells.

4. Optimization of experimental conditions for DNA detection

To obtain the best analytical performance, several parameters, including pH, concentrations of PAF-6 and **P**, and incubation time were investigated, respectively. Finally, the following conditions were determined for the assay: 0.05 mg/mL of PAF-6, 50 nM of **P**, and 4 h of incubation time at 37 °C in pH 7.0 buffer.

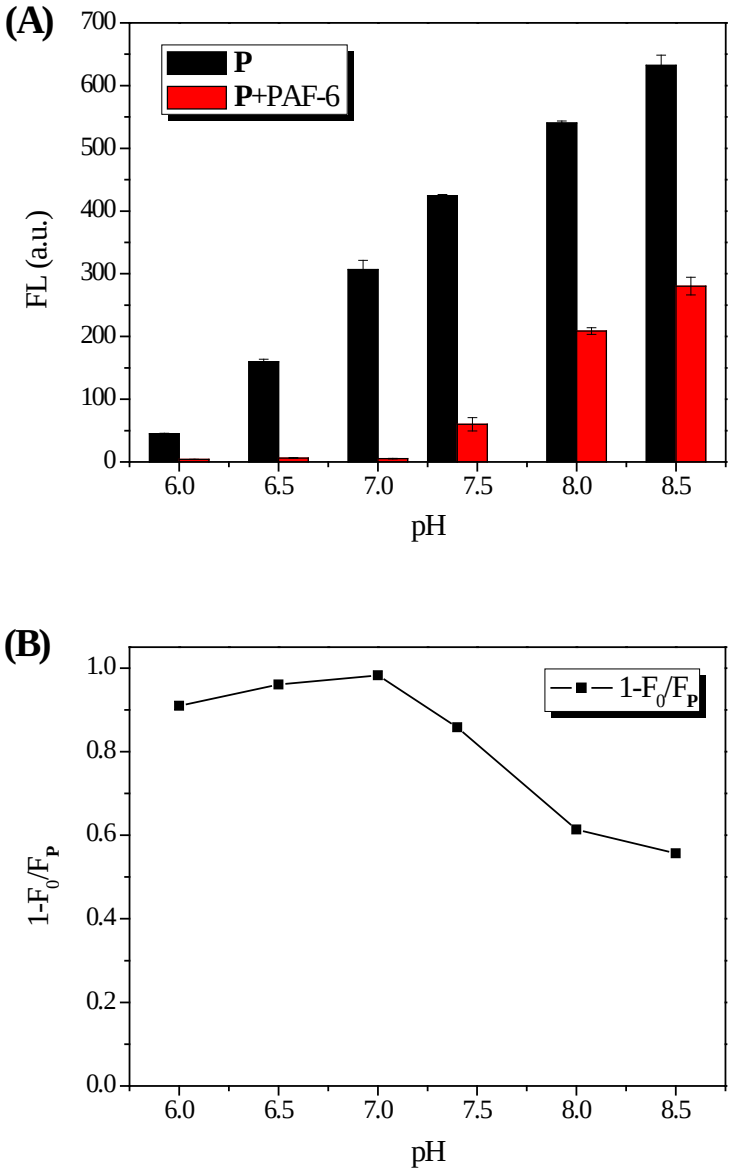

Fig. S6 (A) Fluorescence of **P** in the absence and presence of PAF-6 under different pH conditions and (B) quenching efficiency ($1-F_0/F_{\mathbf{P}}$) under different pH conditions. F_0 and $F_{\mathbf{P}}$ are the fluorescence intensities of **P** at 522 nm in the presence and absence of PAF-6, respectively. [**P**] = 50 nM, [PAF-6] = 0.05 mg/mL. As the quenching efficiency reached maximum at pH 7.0, pH 7.0 was used in subsequent experiments.

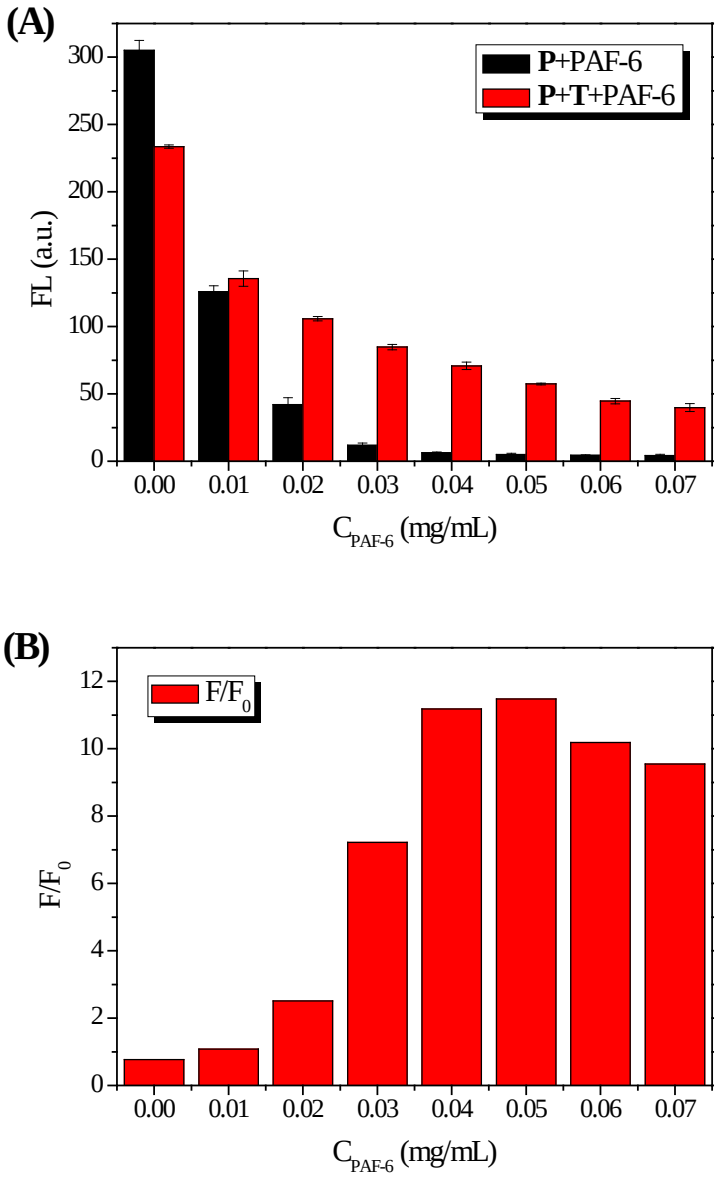

Fig. S7 (A) Fluorescence and (B) signal-to-noise (F/F_0) with different concentrations of PAF-6. F and F_0 are the fluorescence intensities at 522 nm in the presence and absence of **T** after addition of PAF-6, respectively. [**P**] = 50 nM, [**T**] = 50 nM. As the signal-to-noise (F/F_0) reached maximum at 0.05 mg/mL PAF-6, 0.05 mg/mL PAF-6 was used in subsequent experiments.

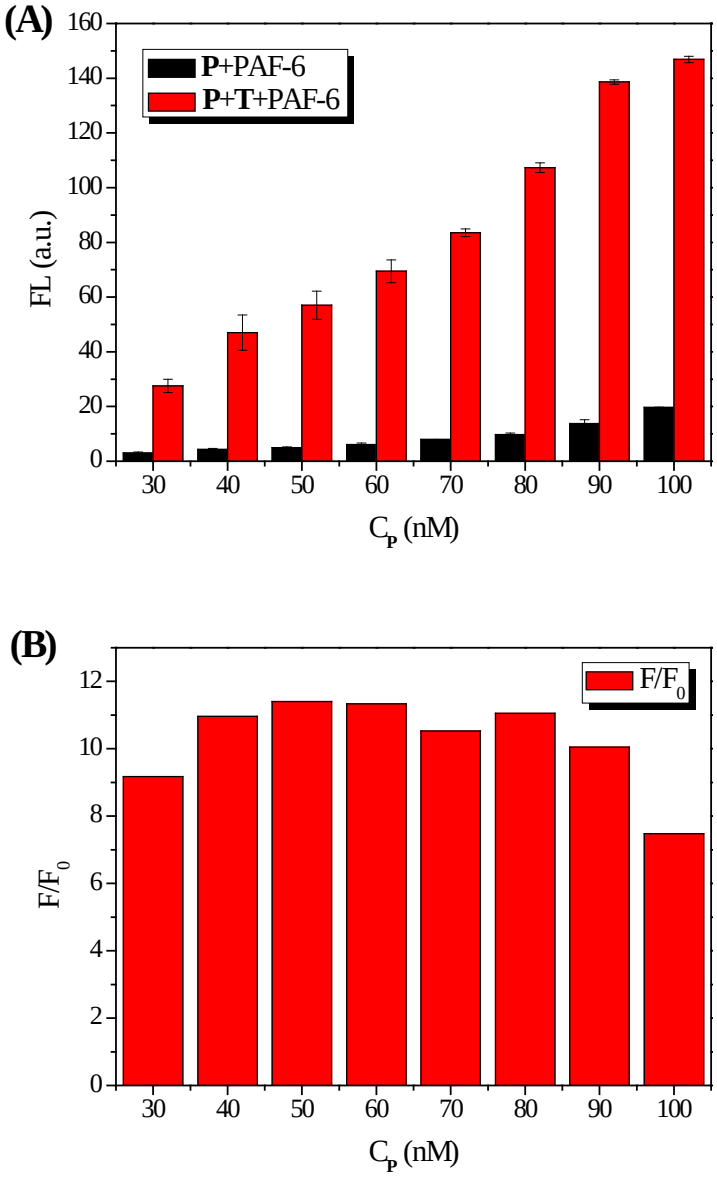

Fig. S8 (A) Fluorescence and (B) signal-to-noise (F/F_0) with different concentrations of **P**. F and F_0 are the fluorescence intensities at 522 nm in the presence and absence of **T** after addition of PAF-6, respectively. [**T**] = 50 nM, [PAF-6] = 0.05 mg/mL. As the signal-to-noise (F/F_0) reached maximum value at 50 nM of **P**, 50 nM **P** was used in subsequent experiments.

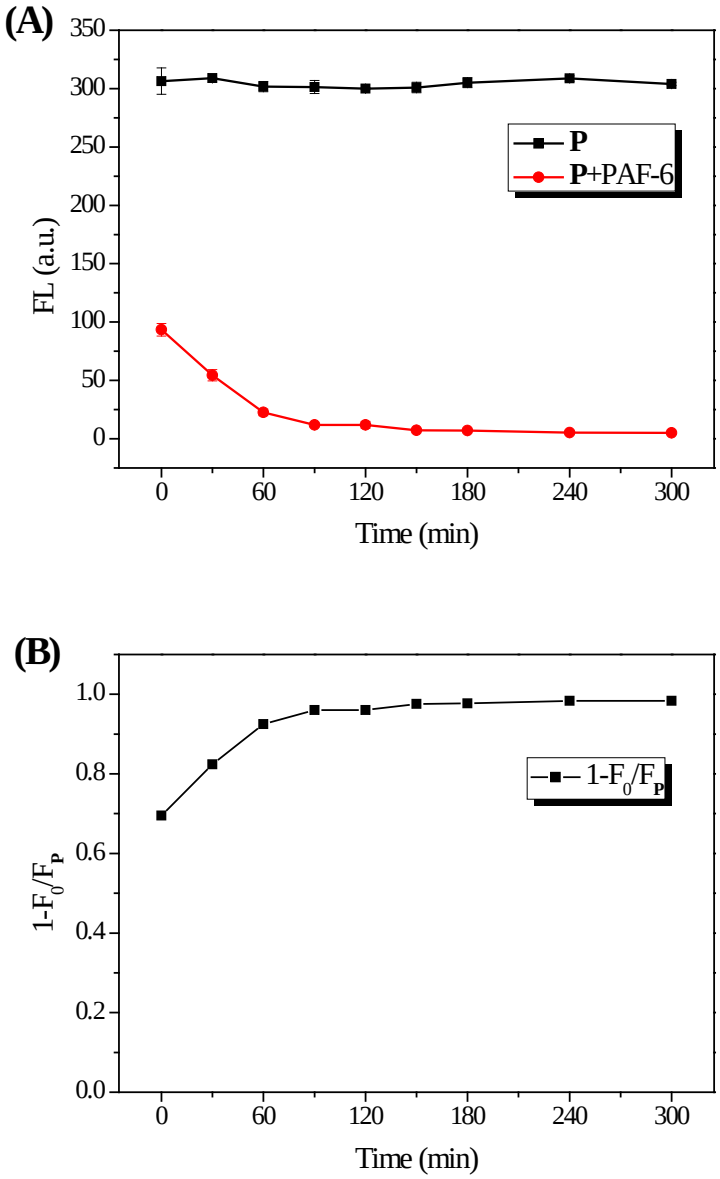

Fig. S9 (A) Fluorescence of **P** in the absence or presence of PAF-6, and (B) quenching efficiency ($1-F_0/F_{\mathbf{P}}$) versus incubation time at 37 °C. The fluorescence intensity of **P** in the presence of PAF-6 at 0 minute was measured after addition of PAF-6 as soon as possible. F_0 and $F_{\mathbf{P}}$ are the fluorescence intensities of **P** at 522 nm in the presence and absence of PAF-6, respectively. [**P**] = 50 nM, [PAF-6] = 0.05 mg/mL.

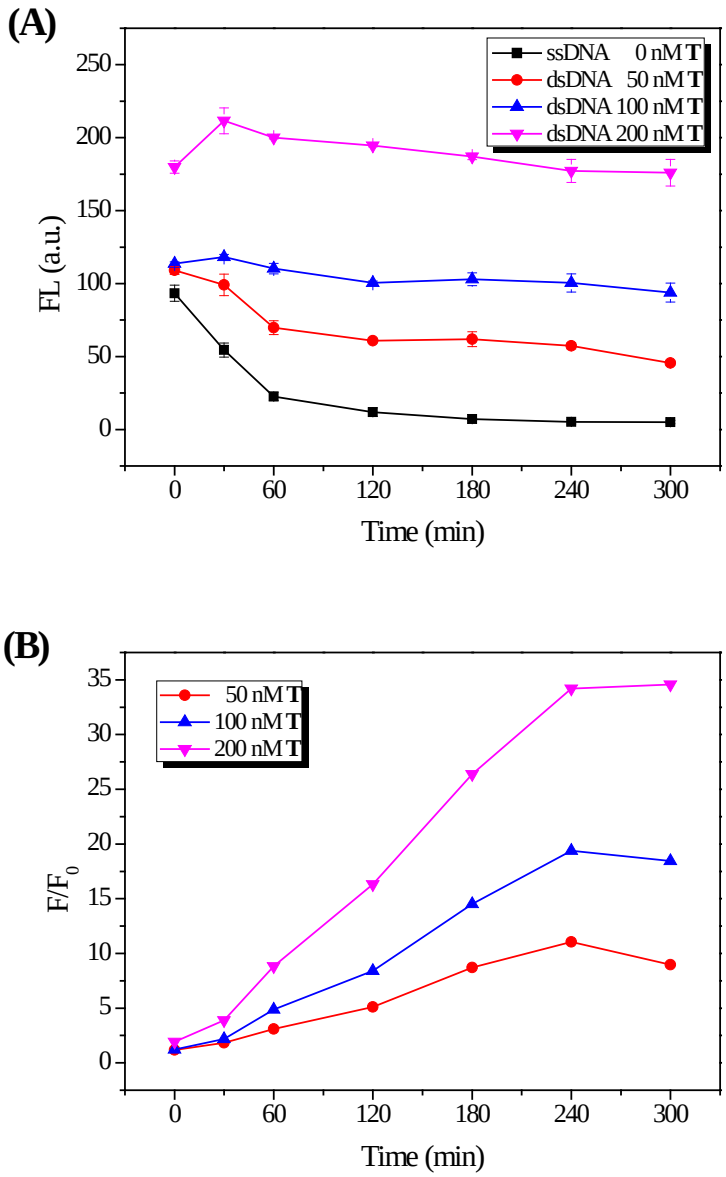

Fig. S10 (A) Fluorescence of **P** in the presence of different concentrations of **T** upon the addition of PAF-6 and (B) their signal-to-noise (F/F_0) versus incubation time at 37 °C. The fluorescence intensities at 0 minute are measured after addition of PAF-6 as soon as possible. F and F_0 are the fluorescence intensities at 522 nm in the presence and absence of **T** after addition of PAF-6, respectively. [**P**] = 50 nM, [PAF-6] = 0.05 mg/mL.

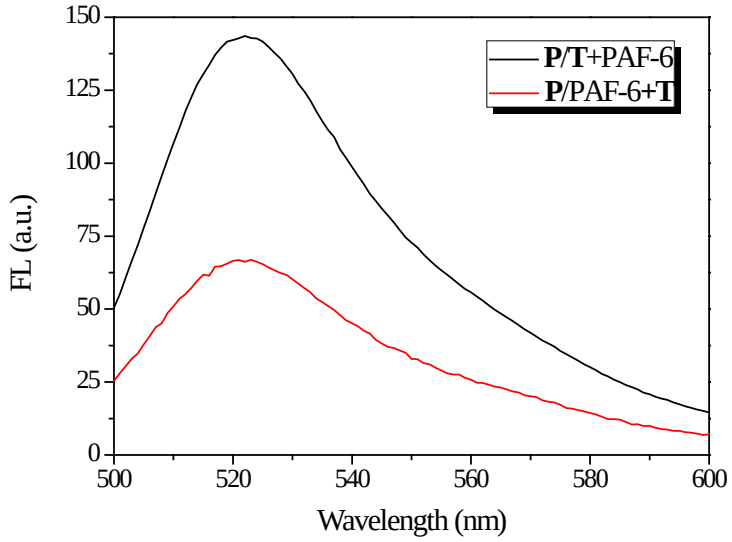

Fig. S11 Effects of reagent addition order on the performance of the DNA-sensing system. [**P**] = 50 nM, [**T**] = 150 nM, [PAF-6] = 0.05 mg/mL.

5. Applications of the nucleic acid-sensing method to sample analysis

Table S2 Recovery of **T** in 1% human serum samples.

Sample	**T** added (M)	Found (nM)	Recovery (%)
1	0	–	–
2	50.0	51.1 ± 1.1	102.2 ± 2.1
3	100.0	101.5 ± 3.9	101.5 ± 3.9
4	150.0	147.1 ± 3.7	98.0 ± 2.5

6. Study on the mechanism for the fluorescence quenching of P by PAF-6

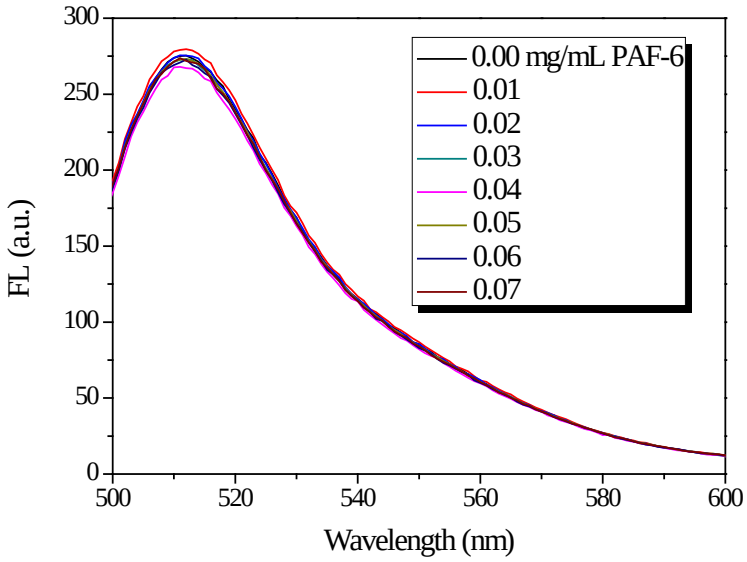

Fig. S12 Fluorescence emission spectra of free fluorescein (FAM) solution (3 nM) in the presence of different concentrations of PAF-6 with an excitation wavelength of 480 nm.

7. UV absorption spectra of PAF-6 in water

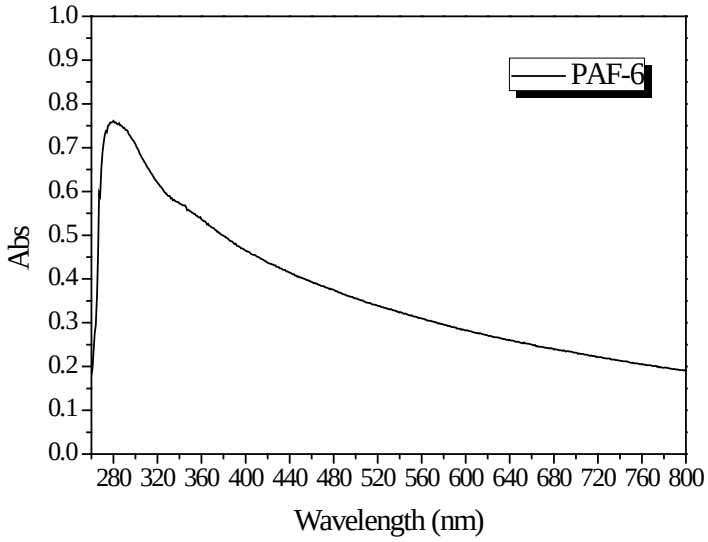

Fig. S13 UV absorption spectra of 0.025 mg/mL PAF-6 in water.

8. Stability study of PAF-6 in solution

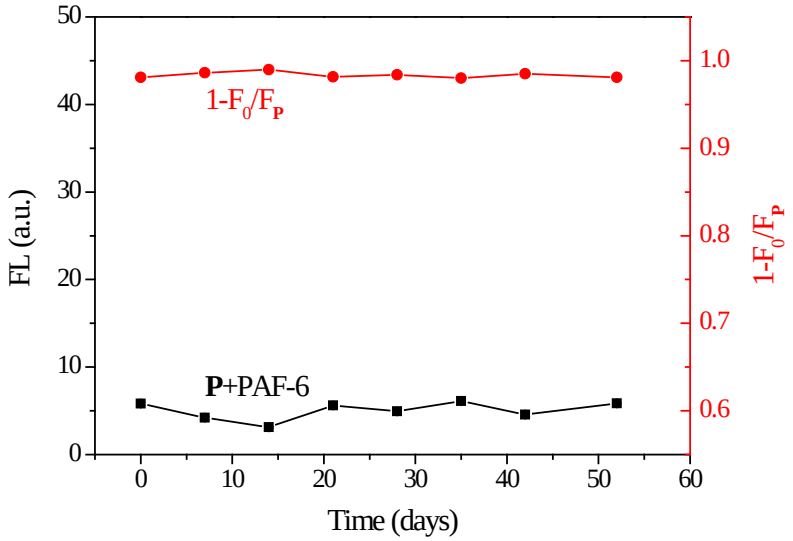

Fig. S14 Fluorescence of **P** in the presence of PAF-6 (black line) and quenching efficiency ($1\text{-}F_0/F_{\mathbf{P}}$) (red line) versus the storage time of the prepared PAF-6. The incubation time of **P** with PAF-6 was 4 h at 37 °C and fluorescence intensity was measured at 522 nm. [**P**] = 50 nM, [PAF-6] = 0.05 mg/mL.

9. Applications of the Exo I activity-sensing method to sample analysis

Table S3 Recovery of Exo I activity in 1% human serum samples.

Sample	Exo I added (U/mL)	Found (U/mL)	Recovery (%)
1	0	–	–
2	3.0	2.8 ± 0.1	93.0 ± 3.8
3	5.0	5.2 ± 0.2	103.3 ± 3.0
4	6.0	5.8 ± 0.2	97.1 ± 3.2